

Pairing: from atomic nuclei to neutron-star crusts

N. Chamel,¹ J. M. Pearson,² and S. Goriely¹

¹*Institut d'Astronomie et d'Astrophysique, CP-226,
Université Libre de Bruxelles, 1050 Brussels, Belgium*

²*Dépt. de Physique, Université de Montréal,
Montréal (Québec), H3C 3J7 Canada*

Abstract

Nuclear pairing is studied both in atomic nuclei and in neutron-star crusts in the unified framework of the energy-density functional theory using generalized Skyrme functionals complemented with a local pairing functional obtained from many-body calculations in homogeneous nuclear matter using realistic forces.

PACS numbers:

I. INTRODUCTION

The possibility of pairing in atomic nuclei was first studied by Bohr, Mottelson and Pines [1] and by Belyaev [2] only one year after the publication of the theory of superconductivity by Bardeen, Cooper and Schrieffer (BCS) [3]. Meanwhile, Bogoliubov developed a microscopic theory of superfluidity and superconductivity and explored its consequences for nuclear matter [4]. In 1959, Migdal speculated that the interior of neutron stars might be superfluid [5] and this scenario was further investigated by Ginzburg and Kirzhnits in 1964 [6]. Soon after the discovery of the first pulsars, the observation of frequency glitches followed by very long relaxation times of the order of months provided strong evidence of nuclear superfluidity [7]. Pulsar glitches are believed to be related to the dynamics of the neutron superfluid permeating the inner layers of the solid neutron star crust [8]. Superfluidity plays also a predominant role in neutron-star cooling (see Page in this volume).

The pairing phenomenon in both finite systems like atomic nuclei and in infinite nuclear matter can be consistently described in the framework of the energy-density functional (EDF) theory (see Dobaczewski and Nazarewicz in this volume). This theory, which has been historically formulated in terms of effective interactions in the context of self-consistent mean-field methods, has been very successful in describing the structure and the dynamics of a wide range of nuclei [9]. These interactions have been also commonly applied to the modeling of neutron-star interiors. Actually no sooner did Skyrme [10] introduce his eponymous effective interaction than Cameron [11] applied it to calculate the structure of neutron stars. By showing that their maximum mass was significantly higher than the Chandrasekhar mass limit, his work brought support to the scenario of neutron star formation from the catastrophic gravitational core-collapse of massive stars during type II supernova explosions, as proposed much earlier by Baade and Zwicky [12].

II. NUCLEAR ENERGY DENSITY FUNCTIONAL THEORY IN A NUTSHELL

Assuming time-reversal symmetry, the ground-state energy E is supposed to depend on (i) the nucleon density (denoting the spin states by $\sigma = \pm 1$ and $q = n$ or p for neutron or

proton, respectively),

$$\rho_q(\mathbf{r}) = \sum_{\sigma=\pm 1} \rho_q(\mathbf{r}, \sigma; \mathbf{r}, \sigma), \quad (1)$$

(ii) the kinetic-energy density (in units of $\hbar^2/2M_q$ where M_q is the nucleon mass),

$$\tau_q(\mathbf{r}) = \sum_{\sigma=\pm 1} \int d^3\mathbf{r}' \delta(\mathbf{r} - \mathbf{r}') \nabla \cdot \nabla' \rho_q(\mathbf{r}, \sigma; \mathbf{r}', \sigma), \quad (2)$$

(iii) the spin-current density,

$$\mathbf{J}_q(\mathbf{r}) = -i \sum_{\sigma, \sigma'=\pm 1} \int d^3\mathbf{r}' \delta(\mathbf{r} - \mathbf{r}') \nabla \rho_q(\mathbf{r}, \sigma; \mathbf{r}', \sigma') \times \hat{\boldsymbol{\sigma}}_{\sigma'\sigma} \quad (3)$$

and (iv) the abnormal density,

$$\tilde{\rho}_q(\mathbf{r}) = \sum_{\sigma=\pm 1} \tilde{\rho}_q(\mathbf{r}, \sigma; \mathbf{r}, \sigma), \quad (4)$$

where $\hat{\boldsymbol{\sigma}}_{\sigma\sigma'}$ denotes the Pauli spin matrices. In turn the normal and abnormal density matrices, $\rho(\mathbf{r}, \sigma; \mathbf{r}', \sigma')$ and $\tilde{\rho}(\mathbf{r}, \sigma; \mathbf{r}', \sigma')$ respectively, can be expressed as

$$\rho_q(\mathbf{r}, \sigma; \mathbf{r}', \sigma') = \sum_{i(q)} \psi_{2i}^{(q)}(\mathbf{r}, \sigma) \psi_{2i}^{(q)*}(\mathbf{r}', \sigma') \quad (5)$$

and

$$\tilde{\rho}_q(\mathbf{r}, \sigma; \mathbf{r}', \sigma') = - \sum_{i(q)} \psi_{1i}^{(q)}(\mathbf{r}, \sigma) \psi_{2i}^{(q)*}(\mathbf{r}', \sigma'), \quad (6)$$

where $\psi_{1i}^{(q)}(\mathbf{r}, \sigma)$ and $\psi_{2i}^{(q)}(\mathbf{r}, \sigma)$ are the two components of the quasiparticle (q.p.) wavefunction. Here, as throughout this paper pure nucleon states are being assumed; the more general formalism involving neutron-proton mixing has been developed in Ref. [13].

Minimizing the total energy E with respect to $\psi_{1i}^{(q)}(\mathbf{r}, \sigma)$ and $\psi_{2i}^{(q)}(\mathbf{r}, \sigma)$ under the constraints of fixed particle numbers leads to the Hartree-Fock-Bogoliubov (HFB) equations¹ (see Dobaczewski and Nazarewicz in this volume)

$$\sum_{\sigma'} \begin{pmatrix} h_q(\mathbf{r})_{\sigma\sigma'} & \Delta_q(\mathbf{r})\delta_{\sigma\sigma'} \\ \Delta_q(\mathbf{r})\delta_{\sigma\sigma'} & -h_q(\mathbf{r})_{\sigma\sigma'} \end{pmatrix} \begin{pmatrix} \psi_{1i}^{(q)}(\mathbf{r}, \sigma') \\ \psi_{2i}^{(q)}(\mathbf{r}, \sigma') \end{pmatrix} = \begin{pmatrix} E_i + \lambda_q & 0 \\ 0 & E_i - \lambda_q \end{pmatrix} \begin{pmatrix} \psi_{1i}^{(q)}(\mathbf{r}, \sigma) \\ \psi_{2i}^{(q)}(\mathbf{r}, \sigma) \end{pmatrix} \quad (7)$$

¹ These equations are also called Bogoliubov-de Gennes equations in condensed matter physics.

where λ_q are Lagrange multipliers. The single-particle (s.p.) Hamiltonian $h_q(\mathbf{r})_{\sigma\sigma'}$ is given by

$$h_q(\mathbf{r})_{\sigma\sigma'} \equiv -\nabla \cdot B_q(\mathbf{r})\nabla \delta_{\sigma\sigma'} + U_q(\mathbf{r})\delta_{\sigma\sigma'} - i\mathbf{W}_q(\mathbf{r}) \cdot \nabla \times \hat{\boldsymbol{\sigma}}_{\sigma\sigma'} \quad (8)$$

with the s.p. fields defined by the functional derivatives

$$B_q(\mathbf{r}) = \frac{\delta E}{\delta \tau_q(\mathbf{r})}, \quad U_q(\mathbf{r}) = \frac{\delta E}{\delta \rho_q(\mathbf{r})}, \quad \mathbf{W}_q(\mathbf{r}) = \frac{\delta E}{\delta \mathbf{J}_q(\mathbf{r})}. \quad (9)$$

Using a local pairing EDF of the form

$$\mathcal{E}_{\text{pair}}(\mathbf{r}) = \frac{1}{4} \sum_{q=n,p} v^{\pi q} [\rho_n(\mathbf{r}), \rho_p(\mathbf{r})] \tilde{\rho}_q(\mathbf{r})^2. \quad (10)$$

the pairing field is given by

$$\Delta_q(\mathbf{r}) = \frac{\delta E}{\delta \tilde{\rho}_q(\mathbf{r})} = \frac{1}{2} v^{\pi q} [\rho_n(\mathbf{r}), \rho_p(\mathbf{r})] \tilde{\rho}_q(\mathbf{r}). \quad (11)$$

Expressions for these fields can be found for instance in Refs. [14, 15]. Eqs. (7)-(11) are still valid at finite temperatures, but Eqs. (5) and (6) will have to be replaced by

$$\begin{aligned} \rho_q(\mathbf{r}, \sigma; \mathbf{r}', \sigma') &= \sum_{i(q)} f_i \psi_{1i}^{(q)}(\mathbf{r}, \sigma) \psi_{1i}^{(q)}(\mathbf{r}', \sigma')^* \\ &+ (1 - f_i) \psi_{2i}^{(q)}(\mathbf{r}, \sigma) \psi_{2i}^{(q)}(\mathbf{r}', \sigma')^* \end{aligned} \quad (12)$$

and

$$\tilde{\rho}_q(\mathbf{r}, \sigma; \mathbf{r}', \sigma') = \sum_{i(q)} (2f_i - 1) \psi_{2i}^{(q)}(\mathbf{r}, \sigma) \psi_{1i}^{(q)}(\mathbf{r}', \sigma')^*, \quad (13)$$

where f_i are the q.p. occupation probabilities given by (setting the Boltzmann constant $k_B = 1$)

$$f_i = \frac{1}{1 + \exp(E_i/T)}. \quad (14)$$

III. SKYRME FUNCTIONALS

The nuclear EDF that we consider here is of the Skyrme type [9], i.e.,

$$E = E_{\text{kin}} + E_{\text{Coul}} + E_{\text{Sky}} + E_{\text{pair}} \quad , \quad (15)$$

where E_{kin} is the kinetic energy of the normalization volume, E_{Coul} is the Coulomb energy (dropping the exchange part in order to simulate neglected effects such as Coulomb correlations, charge-symmetry breaking of the nuclear forces and vacuum polarization as discussed in Ref. [16]), E_{Sky} is the Skyrme energy and E_{pair} is the nuclear pairing energy.

Historically the Skyrme energy was obtained from the Hartree-Fock approximation using an effective interaction of the form [9]

$$\begin{aligned}
v_{i,j}^{\text{Sky}} = & t_0(1 + x_0 P_\sigma) \delta(\mathbf{r}_{ij}) + \frac{1}{2} t_1 (1 + x_1 P_\sigma) \frac{1}{\hbar^2} [p_{ij}^2 \delta(\mathbf{r}_{ij}) + \delta(\mathbf{r}_{ij}) p_{ij}^2] \\
& + t_2 (1 + x_2 P_\sigma) \frac{1}{\hbar^2} \mathbf{p}_{ij} \cdot \delta(\mathbf{r}_{ij}) \mathbf{p}_{ij} + \frac{1}{6} t_3 (1 + x_3 P_\sigma) \rho(\mathbf{r})^\alpha \delta(\mathbf{r}_{ij}) \\
& + \frac{i}{\hbar^2} W_0 (\hat{\boldsymbol{\sigma}}_i + \hat{\boldsymbol{\sigma}}_j) \cdot \mathbf{p}_{ij} \times \delta(\mathbf{r}_{ij}) \mathbf{p}_{ij} \quad ,
\end{aligned} \tag{16}$$

where $\mathbf{r}_{ij} = \mathbf{r}_i - \mathbf{r}_j$, $\mathbf{r} = (\mathbf{r}_i + \mathbf{r}_j)/2$, $\mathbf{p}_{ij} = -i\hbar(\nabla_i - \nabla_j)/2$ is the relative momentum, P_σ is the two-body spin-exchange operator. Likewise, the pairing energy can be obtained from a Skyrme-like effective interaction given by

$$v_{i,j}^{\text{pair}} = \frac{1}{2} (1 - P_\sigma) v^{\pi q} [\rho_n(\mathbf{r}), \rho_p(\mathbf{r})] \delta(\mathbf{r}_{ij}) . \tag{17}$$

Because of the zero-range of the pairing force, a cutoff has to be used in the gap equations in order to avoid divergences (for a review of the various prescriptions, see for instance Ref. [17]).

The density dependence of the pairing strength $v^{\pi q}[\rho_n, \rho_p]$ remains very poorly known. It has been usually assumed that it depends only on the isoscalar density $\rho = \rho_n + \rho_p$ and has often been parametrized as [18]

$$v^{\pi q}[\rho_n, \rho_p] = V_{\pi q}^\Lambda \left(1 - \eta_q \left(\frac{\rho}{\rho_0} \right)^{\alpha_q} \right) , \tag{18}$$

where ρ_0 is the nuclear saturation density while $V_{\pi q}^\Lambda$, η_q and α_q are adjustable parameters. The superscript Λ on $V_{\pi q}^\Lambda$ serves as a reminder that the pairing strength depends very strongly on the cutoff. In principle changing the cutoff modifies also the other parameters but the effects are generally found to be small. Effective interactions with $\eta_q = 0$ ($\eta_q = 1$) have been traditionally referred as volume (surface) pairing. The standard prescription to fix the parameters is to adjust the value of the pairing strength $V_{\pi q}^\Lambda$ to the average gap in ^{120}Sn [19]. However this does not allow an unambiguous determination of the remaining parameters η_q and α_q . Systematic studies of nuclei seem to favor a so-called mixed pairing with $\eta_q \sim 0.5$ and $1/2 \lesssim \alpha_q \lesssim 1$ [20, 21].

The parameters of the Skyrme EDF are usually determined so as to reproduce a set of nuclear data selected according to a specific purpose. The non-uniqueness of the fitting procedure has led to a large number of different parametrizations. Some of them may yield very different predictions when applied outside the domain where they were fitted. This situation is particularly unsatisfactory for nuclear astrophysical applications which require the knowledge of nuclear masses for nuclei so neutron rich that there is no hope of measuring them in the foreseeable future; such nuclei play a vital role in the r-process of nucleosynthesis [22] and are also found in the outer crust of neutron stars [23]. Extrapolations far beyond the neutron drip line are required for the description of the inner crust of neutron stars [24] where nuclear clusters are embedded in a sea of unbound neutrons, which are expected to become superfluid at low enough temperatures. Even though the crust represents only $\sim 1\%$ of the neutron-star mass, it is intimately related to many observed astrophysical phenomena [25]. The need for more reliable extrapolations of these nuclear EDFs has motivated recent efforts to construct non-empirical effective interactions and more generally microscopic nuclear EDFs [26]. Unfortunately such *ab initio* nuclear EDFs have not yet been developed to the point where they can reproduce nuclear data with the same degree of accuracy as do phenomenological EDFs, which can now fit essentially all the nuclear mass data with rms deviations lower than 0.6 MeV [27].

IV. PAIRING IN INFINITE HOMOGENEOUS NUCLEAR MATTER

In infinite homogeneous matter the HFB equations (7) can be readily solved. The q.p. energies are given by

$$E_k^{(q)} = \sqrt{(\varepsilon_k^{(q)} - \lambda_q)^2 + \Delta_q^2}, \quad (19)$$

in terms of the s.p. energies

$$\varepsilon_k^{(q)} = B_q k^2 + U_q. \quad (20)$$

The q.p. wavefunctions reduce to

$$\psi_{1k}^{(q)}(\mathbf{r}, \sigma) = U_k^{(q)} \phi_k(\mathbf{r}, \sigma), \quad \psi_{2k}^{(q)}(\mathbf{r}, \sigma) = V_k^{(q)} \phi_k(\mathbf{r}, \sigma), \quad (21)$$

with

$$U_k^{(q)} = \frac{1}{\sqrt{2}} \left(1 + \frac{\varepsilon_k^{(q)} - \lambda_q}{E_k^{(q)}} \right)^{1/2}, \quad (22)$$

$$V_k^{(q)} = \frac{1}{\sqrt{2}} \left(1 - \frac{\varepsilon_k^{(q)} - \lambda_q}{E_k^{(q)}} \right)^{1/2}, \quad (23)$$

and $\phi_k(\mathbf{r}, \sigma)$ is given by

$$\phi_k(\mathbf{r}, \sigma) \equiv \frac{1}{\sqrt{V}} \exp(i\mathbf{k} \cdot \mathbf{r}) \chi(\sigma), \quad (24)$$

where $\chi(\sigma)$ is the Pauli spinor and V is the normalization volume. The uniform pairing field obeys the well-known isotropic BCS gap equations (see for instance Appendix B of Ref. [14])

$$\Delta_q = -\frac{1}{2} v^{\pi q} [\rho_n, \rho_p] \Delta_q \int_{\Lambda} d\varepsilon \frac{g(\varepsilon)}{E(\varepsilon)} \tanh \frac{E(\varepsilon)}{2T}, \quad (25)$$

where $g(\varepsilon)$ is the density of s.p. states (per unit energy) given by

$$g(\varepsilon) = \frac{1}{4\pi^2} \frac{\sqrt{\varepsilon}}{B_q^{3/2}}. \quad (26)$$

The subscript Λ is to indicate that the integral has to be regularized by introducing a cutoff. We include here all s.p. states whose energy lies below $\lambda_q + \varepsilon_{\Lambda}$ where ε_{Λ} is a pairing energy cutoff.

In the weak-coupling approximation, i.e. $\Delta_q \ll \lambda_q$ and $\Delta_q \ll \varepsilon_{\Lambda}$, it was shown in Ref. [28] that the pairing gap at $T = 0$ is approximately given by

$$\Delta_q(0) = 2\lambda_q \exp\left(\frac{1}{g(\lambda_q)v^{\pi q}}\right) \exp\left[\frac{1}{2}\Lambda\left(\frac{\varepsilon_{\Lambda}}{\lambda_q}\right)\right] \quad (27)$$

where

$$\Lambda(x) = \ln(16x) + 2\sqrt{1+x} - 2\ln\left(1 + \sqrt{1+x}\right) - 4. \quad (28)$$

The Lagrange multiplier λ_q is approximately given by the Fermi energy

$$\lambda_q = B_q k_{Fq}^2, \quad (29)$$

with $k_{Fq} = (3\pi^2\rho_q)^{1/3}$. Note that these expressions were obtained by going beyond the usual “weak-coupling approximation” in which the density of s.p. states is taken as a constant. Even though this provides a good approximation in the case of conventional BCS superconductivity [3], it is less accurate in the nuclear context because many more states are involved in the pairing mechanism. The temperature-dependence of the pairing gap can be very well represented by [29]

$$\Delta_q(T \leq T_c) \simeq \Delta_q(0) \sqrt{1 - \left(\frac{T}{T_c}\right)^{\delta}}, \quad (30)$$

with $\delta \simeq 3.23$ and the critical temperature is given by

$$T_c = \Delta_q(0) \frac{\exp(\zeta)}{\pi} \simeq 0.57 \Delta_q(0). \quad (31)$$

Phenomenological pairing functionals whose parameters have been fitted to nuclei generally yield unrealistic pairing gaps in homogeneous nuclear matter [14, 30]. Given the uncertainties regarding pairing correlations in nuclei, Garrido et al. [31] proposed to determine the parameters of the pairing strength in Eq. (18) by fitting the 1S_0 pairing gaps in infinite symmetric nuclear matter (SNM) as obtained by the realistic Paris potential in the BCS approximation. The pairing interaction between two nucleons inside a nucleus is thus assumed to be locally the same as the pairing interaction between two nucleons in infinite uniform matter. Even though the coupling to surface vibrations is expected to contribute to pairing [32] (see also Kamerdzhev and Avdeenkov in this volume), a local pairing theory seems a reasonable first step (see Bulgac in this volume). The main difficulty of this approach is that because of the highly non-linear character of pairing correlations [33, 34] it is very difficult to guess an appropriate functional form for $v^{\pi q}[\rho_n, \rho_p]$ (see also Lombardo in this volume). For instance, Margueron et al. [35] have recently shown that the parametric form (18) has to be generalized in order to reproduce the 1S_0 pairing gaps in both SNM and pure neutron matter (NeuM) as obtained from Brueckner calculations [36].

Alternatively, Eq. (27) can be inverted to obtain the analytic expression of the pairing strength in terms of a given pairing gap function $\Delta_q(\rho_n, \rho_p)$

$$v^{\pi q}[\rho_n, \rho_p] = -\frac{8\pi^2 B_q^{3/2}}{I_q(\rho_n, \rho_p)} \quad (32)$$

with

$$I_q = \sqrt{\lambda_q} \left[2 \ln \left(\frac{2\lambda_q}{\Delta_q} \right) + \Lambda \left(\frac{\varepsilon_\Lambda}{\lambda_q} \right) \right]. \quad (33)$$

The value of the pairing cutoff ε_Λ is not completely arbitrary and could be fixed as follows. It has been argued [31, 37] that in the limit $\rho \rightarrow 0$, the pairing strength should coincide with the bare force in the 1S_0 channel, which in turn is determined by the experimental 1S_0 nucleon-nucleon phase shifts. However at very low densities, the pairing strength is simply given by

$$v^{\pi q}[\rho \rightarrow 0] = -\frac{4\pi^2}{\sqrt{\varepsilon_\Lambda}} \left(\frac{\hbar^2}{2M_q} \right)^{3/2}. \quad (34)$$

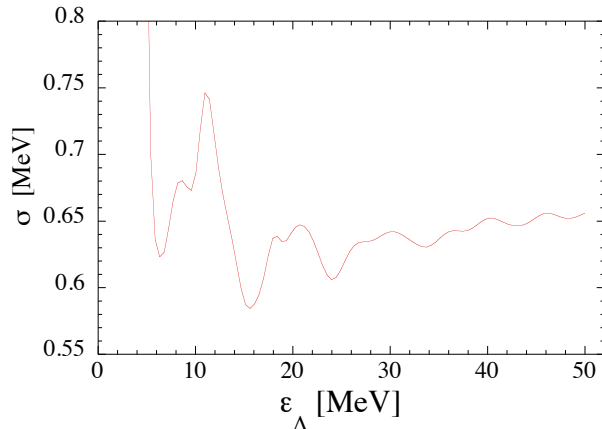


FIG. 1: Root mean square deviation σ between theoretical and experimental masses for some 260 known spherical or quasi-spherical nuclei for different values of the pairing cut-off energies. See text for more details.

The optimal value of the cutoff is thus found to be $\varepsilon_{\Lambda} \sim 7 - 8$ MeV (note that ε_{Λ} is half the cutoff used in Ref. [37]). On the other hand, such a low cutoff may not be optimal in applications to finite nuclei. As seen in Fig. 1, the root mean square (rms) deviation obtained with respect to about 260 known masses of (quasi-)spherical nuclei is found to oscillate as a function of the cutoff energy with clear minima lying around 7, 16 and 24 MeV. In this example, the initial EDF has the same characteristics as BSk21 with a pairing functional constrained on nuclear matter properties [27], as described in the next section. Note that for each value of the cut-off, the Skyrme interaction parameters were re-adjusted to minimize the rms deviation. In particular, we found systematically that global fits to nuclear masses favor $\varepsilon_{\Lambda} \sim 16$ MeV, a value which we adopted. Similar results were obtained when considering a traditional δ -pairing force with or without the Bulgac-Yu regularization [38].

V. PAIRING IN NUCLEI

We have recently constructed a family of three nuclear EDFs, BSk19, BSk20 and BSk21 [27] based on Skyrme forces that are generalized in the sense that they contain density-dependent generalizations of the usual t_1 and t_2 terms, respectively [15]. The neutron-pairing functional was obtained from Eqs. (32)-(33) using the 1S_0 pairing gaps both in SNM matter and NeM, as obtained from Brueckner calculations including medium polarization ef-

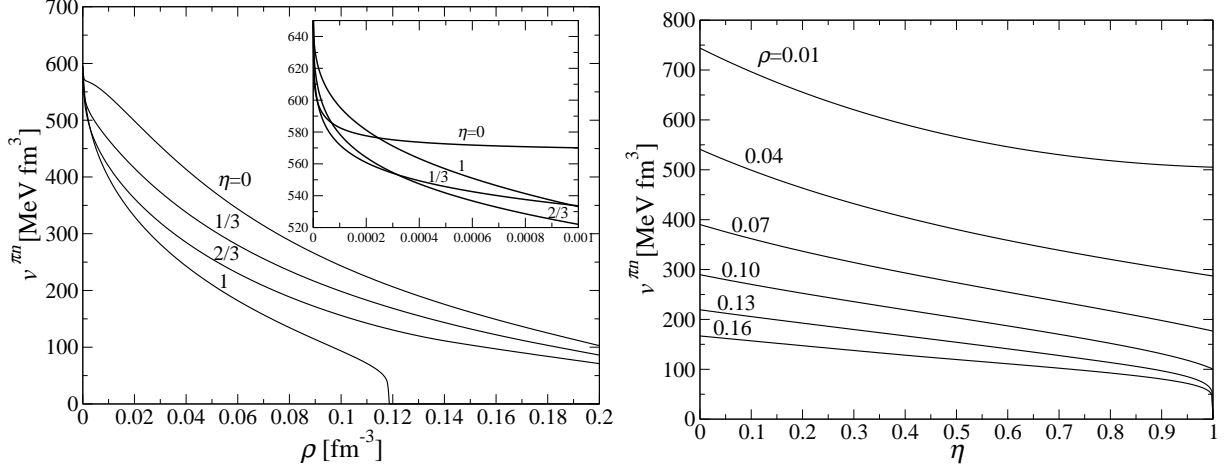


FIG. 2: Neutron pairing strength as a function of the nucleon density $\rho = \rho_n + \rho_p$ and isospin asymmetry $\eta = (\rho_n - \rho_p)/\rho$.

fects [36]. The resulting pairing strength is shown in Fig. 2. The proton-pairing functional had the same form but we allowed its strength to be different from the neutron-pairing strength in order to take account of Coulomb effects not included in the above nuclear matter calculations. Because of our neglect of polarization effects in odd nuclei due to our use of the equal-filling approximation [39], we also allowed each of these strengths to depend on whether there is an even or odd number of nucleons of the charge type in question². These extra degrees of freedom were taken into account by multiplying the neutron-pairing functional $v^{\pi q}[\rho_n, \rho_p]$, as determined by the nuclear-matter calculations that we have just described, with renormalizing factors f_q^\pm , where f_p^+ , f_p^- and f_n^- are free, density-independent parameters to be included in the mass fit, with f_n^+ set equal to 1.

The remaining parameters of the functionals were determined primarily by fitting essentially all measured nuclear masses. For this it was necessary to add two phenomenological corrections to the HFB ground-state energy: (i) a Wigner energy (which contributes significantly only for light nuclei or nuclei with N close to Z) and (ii) a correction for the spurious rotational and vibrational collective energy. However, in fitting the mass data we simultaneously constrained the functional to fit the zero-temperature equation of state (EOS) of NeUM, as determined by three different many-body calculations using realistic two- and three-nucleon forces. Finally, we imposed on these EDFs the supplementary constraints

² Note that the odd nucleon will nevertheless contribute to the time-even fields.

of i) eliminating all spurious spin-isospin instabilities in nuclear matter both at zero and finite temperatures, at all densities found in neutron stars and supernova cores [15, 27, 40], ii) obtaining a qualitatively realistic distribution of the potential energy among the four spin-isospin channels in nuclear matter, iii) ensuring that the isovector effective mass is smaller than the isoscalar effective mass, as indicated by both experiments and many-body calculations and iv) restricting the incompressibility coefficient of SNM to lie in the range $K_v = 240 \pm 10$ MeV, as inferred from breathing-mode measurements.

The introduction of the unconventional Skyrme terms allowed us to satisfy all these constraints and at the same time fit the 2149 measured masses of nuclei with N and $Z \geq 8$ given in the 2003 Atomic Mass Evaluation (AME) [41] with an rms deviation as low as 0.58 MeV for all three EDFs. Incidentally, our EDFs are found to be consistent with measurements of the high-density pressure of SNM deduced from heavy-ion collisions [42], even though they were not directly fitted to the EOS of SNM.

VI. PAIRING IN NEUTRON-STAR CRUSTS

Because of the precision fit to masses and the constraints on both the EOS and the 1S_0 pairing gaps in NeuM, our recently developed EDFs BSk19, BSk20 and BSk21 [27] are particularly well-suited for describing the inner crust of neutron stars.

The HFB equations (7) have been already solved in neutron-star crusts using the so-called Wigner-Seitz (W-S) approximation according to which the crust is divided into a set of independent spheres centered around each lattice site [43–45] (see also Barranco et al. in this volume). However this way of implementing the HFB method can only be reliably applied in the shallowest region of the inner crust where nuclear clusters are very far apart [46]. In order to investigate pairing correlations in the densest part of the crust, we have applied the band theory of solids, which takes into account both short- and long-range correlations [47]. The band theory relies on the assumption that the solid crust can be treated as a perfect crystal, which is a reasonable approximation for cold non-accreting neutron stars [25]. According to the Floquet-Bloch theorem, the q.p. wave function must obey the following boundary conditions [48] for any lattice translation vectors $\boldsymbol{\ell}$

$$\begin{aligned}\psi_{1\alpha\mathbf{k}}^{(q)}(\mathbf{r} + \boldsymbol{\ell}, \sigma) &= \exp(i\mathbf{k} \cdot \boldsymbol{\ell}) \psi_{1\alpha\mathbf{k}}^{(q)}(\mathbf{r}, \sigma) \\ \psi_{2\alpha\mathbf{k}}^{(q)}(\mathbf{r} + \boldsymbol{\ell}, \sigma) &= \exp(i\mathbf{k} \cdot \boldsymbol{\ell}) \psi_{2\alpha\mathbf{k}}^{(q)}(\mathbf{r}, \sigma)\end{aligned}\tag{35}$$

where α is the band index (principal quantum number) and \mathbf{k} the Bloch wave vector. This formalism naturally incorporates the local rotational symmetries around the nuclear clusters as well as the translational symmetry of the lattice, thus describing consistently both clusters and superfluid neutrons. Note that this formalism also includes infinite homogeneous matter as the limiting case of an “empty” lattice. The band theory therefore allows for a unified treatment of all regions of a neutron star.

In the deep layers of the inner crust of a neutron star, where spatial inhomogeneities are small, further simplifications can be made. In the decoupling approximation, the q.p. wavefunction is expressed in terms of the s.p. wavefunctions $\varphi_{\alpha\mathbf{k}}^{(q)}$ as

$$\psi_{1\alpha\mathbf{k}}^{(q)}(\mathbf{r}, \sigma) = U_{\alpha\mathbf{k}}^{(q)} \varphi_{\alpha\mathbf{k}}^{(q)}(\mathbf{r}, \sigma), \quad \psi_{2\alpha\mathbf{k}}^{(q)}(\mathbf{r}, \sigma) = V_{\alpha\mathbf{k}}^{(q)} \varphi_{\alpha\mathbf{k}}^{(q)}(\mathbf{r}, \sigma). \quad (36)$$

The HFB equations can then be readily solved, and the q.p. energies are given by

$$E_{\alpha\mathbf{k}}^{(q)} = \sqrt{(\varepsilon_{\alpha\mathbf{k}}^{(q)} - \lambda_q)^2 + (\Delta_{\alpha\mathbf{k}}^{(q)})^2} \quad (37)$$

where $\varepsilon_{\alpha\mathbf{k}}^{(q)}$ are the s.p. energies and $\Delta_{\alpha\mathbf{k}}^{(q)}$ are solutions of the anisotropic multi-band BCS gap equations [47]

$$\Delta_{\alpha\mathbf{k}}^{(q)} = -\frac{V}{2} \sum_{\beta} \int \frac{d^3\mathbf{k}'}{(2\pi)^3} V_{\alpha\mathbf{k}\beta\mathbf{k}'}^{(q)} \frac{\Delta_{\beta\mathbf{k}'}^{(q)}}{E_{\beta\mathbf{k}'}^{(q)}} \tanh \frac{E_{\beta\mathbf{k}'}^{(q)}}{2T}. \quad (38)$$

with

$$V_{\alpha\mathbf{k}\beta\mathbf{k}'}^{(q)} = \int_{\text{WS}} d^3r v^{\pi q} [\rho_n(\mathbf{r}), \rho_p(\mathbf{r})] |\varphi_{\alpha\mathbf{k}}^{(q)}(\mathbf{r})|^2 |\varphi_{\beta\mathbf{k}'}^{(q)}(\mathbf{r})|^2. \quad (39)$$

The subscript WS indicates that the integral has to be taken inside the W-S cell. Finally the amplitudes of the q.p. wavefunction are given by

$$U_{\alpha\mathbf{k}}^{(q)} = \frac{1}{\sqrt{2}} \left(1 + \frac{\varepsilon_{\alpha\mathbf{k}}^{(q)} - \lambda_q}{E_{\alpha\mathbf{k}}^{(q)}} \right)^{1/2}, \quad (40)$$

$$V_{\alpha\mathbf{k}}^{(q)} = \frac{1}{\sqrt{2}} \left(1 - \frac{\varepsilon_{\alpha\mathbf{k}}^{(q)} - \lambda_q}{E_{\alpha\mathbf{k}}^{(q)}} \right)^{1/2}. \quad (41)$$

We have solved Eq. (38) for neutrons in the deep region of neutron-star crusts as described in Ref. [47] using our latest BSk21 EDF (which is strongly favored by the most recent atomic mass data while being also consistent with what is now known about neutron-star

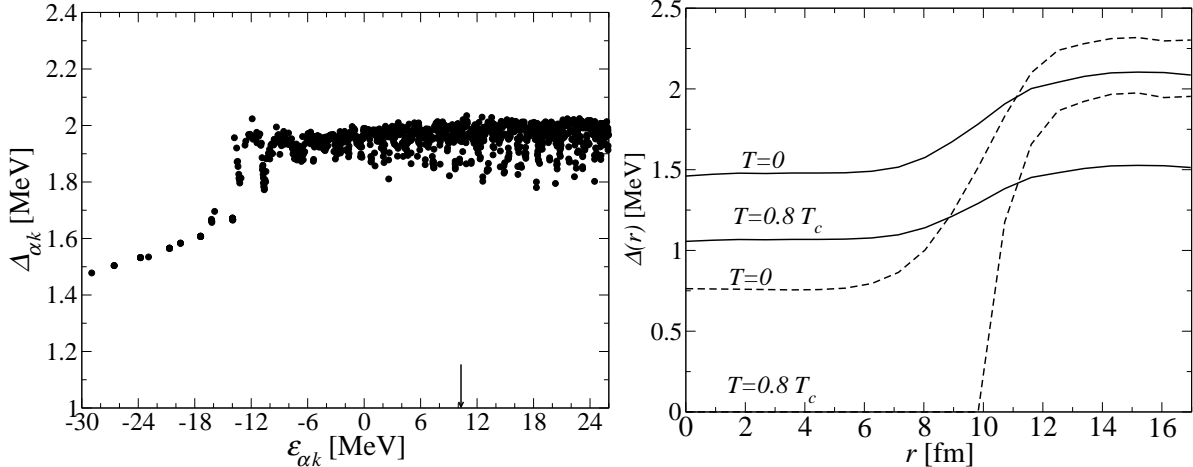


FIG. 3: Neutron superfluidity in neutron-star crust at average baryon density $\bar{\rho} = 0.06 \text{ fm}^{-3}$ with BSk21. The critical temperature is found to be equal to $T_c = 1.1 \text{ MeV}$. Left panel: pairing gaps vs single-particle energies at $T = 0$. The arrow indicates the position of the Fermi energy. Right panel: pairing field in the W-S cell obtained from the HFB equations (solid line) and from the LDA (dashed line) for two different temperatures.

masses [49]). Due to the presence of the nuclear clusters, neutrons belonging to different bands and having different Bloch wave vectors feel different pairing interactions thus leading to a dispersion of the neutron pairing gaps $\Delta_{\alpha\mathbf{k}}^{(n)}$ of a few hundred keV around the Fermi level, as shown in Fig. 3. The critical temperature is found to be very weakly dependent on the cutoff, as can be seen in Table I (note that ε_{Λ} was varied while using the *same* Skyrme functional BSk21).

Because the neutron superfluid coherence length is much larger than the size of the clusters, proximity effects are very strong. As a result, pairing correlations are substantially enhanced inside clusters while they are reduced in the interstitial region, leading to a smooth spatial variation of the pairing field. The local density approximation (LDA), whereby the neutron pairing field $\Delta_n(\mathbf{r})$ is assumed to be locally the same as that in uniform nuclear matter for the neutron density $\rho_n(\mathbf{r})$ and proton density $\rho_p(\mathbf{r})$, strongly overestimates the spatial variations of the pairing field. The discrepancies are particularly large inside clusters where the LDA incorrectly predicts a quenching of pairing correlations, especially for temperatures close to the critical temperature as illustrated in Fig. 3. This analysis shows that a consistent treatment of both unbound neutrons and nucleons bound in clusters is essential

TABLE I: Cut-off dependence of the critical temperature of neutron superfluidity in neutron star crusts at density $\bar{\rho} = 0.06 \text{ fm}^{-3}$ with BSk21. See text for further details.

ε_{Λ} [MeV]	2	4	8	16	32
T_c [MeV]	1.10	1.06	1.07	1.11	1.16

for a realistic description of pairing correlations in neutron-star crusts.

Despite the absence of viscous drag at $T = 0$, the solid crust can still resist the flow of the neutron superfluid due to non-dissipative entrainment effects. These effects have been systematically studied in all regions of the inner crust of a cold non-accreting neutron star [50]. In particular, it has been found that in some layers of the inner crust, almost all neutrons are entrained by clusters. These results suggest that a revision of the interpretation of many observable astrophysical phenomena like pulsar glitches might be necessary [51].

VII. CONCLUSIONS

The nuclear EDF theory opens the way to a unified description of the nuclear pairing phenomenon in various systems, from atomic nuclei to neutron stars.

The Brussels-Montreal EDFs based on generalized Skyrme EDFs supplemented by a microscopic local pairing EDF yield an excellent fit to essentially all experimental nuclear mass data with rms deviations falling below 0.6 MeV, while reproducing at the same time many-body calculations in infinite homogeneous nuclear matter using realistic forces. For this reason, these EDFs are particularly well-suited for studying pairing correlations in the inner crust of neutron stars, where nuclear clusters are expected to coexist with a neutron superfluid.

Despite these successes, a number of open issues like for instance neutron-proton pairing or the contribution of surface vibrations to pairing call for more elaborate pairing EDFs.

-
- [1] A. Bohr, B. R. Mottelson, and D. Pines, Phys. Rev. **110**, 936 (1958).
 - [2] S.T. Belyaev, Mat.-Fys. Medd. K. Dan. Vid. Selsk. 31 , 11 (1959).
 - [3] J. Bardeen, L. N. Cooper, and J. R. Schrieffer, Phys. Rev. **108**, 1175 (1957).

- [4] N. N. Bogoliubov, Dokl. Ak. nauk SSSR 119, 52 (1958).
- [5] A. B. Migdal, Nucl. Phys. **13**, 655 (1959).
- [6] V. L. Ginzburg and D.A. Kirzhnits, Zh. Eksp. Teor. Fiz. 47, 2006, (1964).
- [7] G. Baym, C. J. Pethick, and D. Pines, Nature **224**, 673 (1969).
- [8] P. W. Anderson and N. Itoh, Nature **256**, 25 (1975).
- [9] M. Bender, P.-H. Heenen and P.-G. Reinhard, Rev. Mod. Phys. **75**, 121 (2003).
- [10] T. H. R. Skyrme, Nucl. Phys. **9**, 615 (1959).
- [11] A. G. W. Cameron, ApJ **130**, 884 (1959).
- [12] W. Baade and F. Zwicky, Phys. Rev. **45**, 138 (1933).
- [13] E. Perlińska, S.G. Rohoziński, J. Dobaczewski, W. Nazarewicz, Phys. Rev. **C69**, 014316 (2004).
- [14] N. Chamel, S. Goriely, and J. M. Pearson, Nucl. Phys. **A812**, 72 (2008).
- [15] N. Chamel, S. Goriely, and J. M. Pearson, Phys. Rev. C **80**, 065804 (2009).
- [16] S.Goriely and J.M. Pearson, Phys. Rev. C **77**, 031301 (2008).
- [17] T. Duguet, K. Bennaceur, P. Bonche, nucl-th/0508054, in Proceedings of the YITP Workshop on New Developments in Nuclear Self-Consistent Mean-Field Theories, Kyoto, 2005 (YITP-W-05-01), p. B20.
- [18] G. F. Bertsch and H. Esbensen, Ann. Phys. **209**, 327 (1991).
- [19] J. Dobaczewski, W. Nazarewicz, and T. Werner, Phys. Scr. **T56**, 15 (1995).
- [20] J. Dobaczewski, W. Nazarewicz, P.-G. Reinhard, Nucl. Phys. **A693**, 361 (2001).
- [21] M. Samyn, S. Goriely, J.M. Pearson, Nucl. Phys. **A725** (2003) 69.
- [22] M. Arnould, S. Goriely, K. Takahashi, Phys. Rep. **450**, 97 (2007).
- [23] J.M. Pearson, S. Goriely, N. Chamel, M. Samyn, M. Onsi, AIP Conf. Proc.1128(2009),29.
- [24] M. Onsi, A. K. Dutta, H. Chatri, S. Goriely, N. Chamel, J. M. Pearson, Phys. Rev. C **77**, 065805 (2008).
- [25] N. Chamel and P. Haensel, "Physics of Neutron Star Crusts", Living Rev. Relativity 11, (2008), 10. <http://www.livingreviews.org/lrr-2008-10>
- [26] J. E. Drut, R. J. Furnstahl, L. Platter, Prog. Part. Nucl. Phys. **64**, 120 (2010).
- [27] S. Goriely, N. Chamel, and J. M. Pearson, Phys. Rev. C **82**, 035804 (2010).
- [28] N. Chamel, Phys. Rev. C **82**, 014313 (2010).
- [29] S. Goriely, Nucl. Phys. **A605**, 28 (1996).

- [30] S. Takahara, N. Onishi, N. Tajima, Phys. Lett. B **331**, 261 (1994).
- [31] E. Garrido, P. Sarriguren, E. Moya de Guerra, P. Schuck, Phys. Rev.C **60** (1999), 064312.
- [32] D.M. Brink and R.A. Broglia, Nuclear Superfluidity, Cambridge University Press (2005).
- [33] T. Duguet, Phys. Rev. C **69**, 054317 (2004).
- [34] S.S. Zhang, L.G. Cao, U. Lombardo, E.G. Zhao, S.G. Zhou, Phys. Rev. C **81**, 044313 (2010).
- [35] J. Margueron, H. Sagawa and K. Hagino, Phys. Rev. C **77**, 054309 (2008).
- [36] L.G. Cao, U.Lombardo, and P.Schuck, Phys. Rev. C **74**, 064301 (2006).
- [37] H. Esbensen, G.F. Bertsch and K. Hencken, Phys. Rev. C **56**, 3054 (1997).
- [38] S. Goriely, M. Samyn, J.M. Pearson, Nucl. Phys. **A773** (2006) 279.
- [39] S. Perez-Martin and L. M. Robledo, Phys. Rev. C **78**, 014304 (2008).
- [40] N. Chamel, S. Goriely, Phys. Rev. C **82**, 045804 (2010).
- [41] G. Audi, A.H. Wapstra, and C. Thibault, Nucl. Phys. **A729**, 337 (2003).
- [42] P. Danielewicz, R. Lacey, and W.G. Lynch, Science **298**, 1592 (2002).
- [43] M. Baldo, E. E. Saperstein and S. V. Tolokonnikov, Phys. Rev. C **76**, 025803 (2007).
- [44] F. Grill, J. Margueron, and N. Sandulescu, Phys. Rev. C **84**, 065801 (2011).
- [45] A. Pastore, S. Baroni, and C. Losa, Phys. Rev. C **84**, 065807 (2011).
- [46] N. Chamel, S. Naimi, E. Khan and J. Margueron, Phys. Rev. C **75**, 055806 (2007).
- [47] N. Chamel, S. Goriely, J.M. Pearson and M. Onsi, Phys. Rev. C **81**, 045804 (2010).
- [48] W.N. Mathews Jr., Z. Phys. B **24**, 371 (1976).
- [49] N. Chamel, A. F. Fantina, J. M. Pearson, and S. Goriely, Phys. Rev. C **84**, 062802(R) (2011).
- [50] N. Chamel, Phys. Rev. C **85**, 035801 (2012).
- [51] N. Chamel and B. Carter, Mon.Not.Roy.Astron.Soc. **368**, 796 (2006).